# Self-Assembly of Aβ1−42 into Globular Neurotoxins

**ARTICLE** *in* BIOCHEMISTRY · DECEMBER 2003

Impact Factor: 3.02 · DOI: 10.1021/bi030029q · Source: PubMed

# Self-Assembly of A$\beta_{1-42}$ into Globular Neurotoxins[†]

Brett A. Chromy,[‡] Richard J. Nowak,[#] Mary P. Lambert,[⊥] Kirsten L. Viola,[⊥] Lei Chang,[⊥] Pauline T. Velasco,[⊥] Bryan W. Jones,[⊥] Sara J. Fernandez,[⊥] Pascale N. Lacor,[⊥] Peleg Horowitz,[§] Caleb E. Finch,[∥] Grant A. Krafft,[▽] and William L. Klein*[,⊥]

*Biodefense Division, Biology and Biotechnology Research Program, Lawrence Livermore National Laboratory, 7000 East Avenue, L-446, Livermore, California 94551, Department of Neurology, Harvard Medical School, 65 Landsdowne Street, Cambridge, Massachusetts 02139, Department of Neurobiology and Physiology, 2205 Tech Drive, Northwestern University, Evanston, Illinois 60208, Medical School, Northwestern University, 320 East Superior Street, Chicago, Illinois 60611, Andrus Gerontology Center, University of Southern California, Los Angeles, California 90089, and Acumen Pharmaceuticals, 1309 Evergreen Ct, Glenview, Illinois 60025*

*Received February 3, 2003*

ABSTRACT: Amyloid $\beta$ 1−42 (A$\beta_{1-42}$) is a self-associating peptide that becomes neurotoxic upon aggregation. Toxicity originally was attributed to the presence of large, readily formed A$\beta$ fibrils, but a variety of other toxic species are now known. The current study shows that A$\beta_{1-42}$ can self-assemble into small, stable globular assemblies free of fibrils and protofibrils. Absence of large molecules was verified by atomic force microscopy (AFM) and nondenaturing gel electrophoresis. Denaturing electrophoresis revealed that the globular assemblies comprised oligomers ranging from trimers to 24mers. Oligomers prepared at 4 °C stayed fibril-free for days and remained so when shifted to 37 °C, although the spectrum of sizes shifted toward larger oligomers at the higher temperature. The soluble, globular A$\beta_{1-42}$ oligomers were toxic to PC12 cells, impairing reduction of MTT and interfering with ERK and Rac signal transduction. Occasionally, oligomers were neither toxic nor recognized by toxicity-neutralizing antibodies, suggesting that oligomers could assume alternative conformations. Tests for oligomerization-blocking activity were carried out by dot-blot immunoassays and showed that neuroprotective extracts of *Ginkgo biloba* could inhibit oligomer formation at very low doses. The observed neurotoxicity, structure, and stability of synthetic A$\beta_{1-42}$ globular assemblies support the hypothesis that A$\beta_{1-42}$ oligomers play a role in triggering nerve cell dysfunction and death in Alzheimer's disease.

Alzheimer's disease (AD)[1] is a fatal progressive dementia characterized pathologically by protein-based hallmarks known as neurofibrillary tangles and amyloid plaques. The major constituents of tangles and plaques are large fibrillar molecules generated, respectively, from hyperphosphorylated tau and amyloid beta (A$\beta$), an amphipathic peptide comprising 39−43 amino acids and derived by complex proteolysis from a membrane protein precursor (reviewed in refs *1* and *2*). Pathogenesis has been linked to accumulation of the highly amyloidogenic A$\beta_{1-42}$, whose production is fostered by AD-promoting mutations and risk factors (*3*).

Preparations made from synthetic A$\beta$ are capable of killing neurons in cell culture. Activity requires peptide self-association (*4*−*6*), as solutions of monomeric A$\beta$ are at first innocuous but with time develop neurotoxicity. Neurotoxic preparations typically examined by electron microscopy exhibit conspicuous, large amyloid fibrils, similar to those observed in AD senile plaques. Neurotoxicity of amyloid fibrils initially was taken as the basis for the amyloid cascade, the most prominent hypothesis for Alzheimer's pathogenesis (*7*). However, subsequent studies have shown that neurological dysfunction and degeneration can be linked to much smaller, soluble assemblies of A$\beta$ (*8*−*10*), which now have been incorporated into a revised version of the amyloid cascade hypothesis (*11*).

The initial indication that small, nonfibrillar A$\beta$ structures might be germane to AD pathogenesis was the observation that apolipoprotein J (apoJ) increased the metabolic impact of A$\beta_{1-42}$ solutions on PC12 cells despite blocking large fibril formation (*12*). Subsequent analyses showed that apoJ fostered formation of small globular oligomers of A$\beta_{1-42}$, which have been referred to as ADDLs (*8*). ADDLs are potent CNS neurotoxins that rapidly inhibit hippocampal long-term potentiation (LTP), a classic model for CNS synaptic plasticity. Over longer periods, low concentrations

[†] This work is supported by funding from the NIH (RO1-AG18877 and PO1-AG15501), the Boothroyd, Feiger, and French Foundations, the Institute for the Study of Aging, and a benefactor of Northwestern University.

* To whom correspondence should be addressed: Telephone (847) 491−5510. E-mail: wklein@northwestern.edu.

[‡] Lawrence Livermore National Laboratory.

[#] Harvard Medical School.

[⊥] Department of Neurobiology and Physiology, Northwestern University.

[§] Medical School, Northwestern University.

[∥] Andrus Gerontology Center, University of Southern California.

[▽] Acumen Pharmaceuticals.

[1] Abbreviations: A$\beta$, amyloid beta peptide; AD, Alzheimer's disease; ADDLs, A$\beta$-derived diffusible ligands; AFM, atomic force microscopy; apoJ, apolipoprotein J; BSA, bovine serum albumin; DMSO, dimethyl sulfoxide; HFIP, 1,1,1,3,3,3-hexafluoro-2-propanol; MTT, 3-(4,5-dimethyl-2-thiazolyl)-2,5-diphenyl-2H-tetrazolium bromide; NGF, nerve growth factor; PC12, PC12 rat pheochromacytoma cells; SDS−PAGE, sodium dodecyl sulfate−polyacrylamide gel electrophoresis.

10.1021/bi030029q CCC: $25.00 
Published on Web 10/17/2003

of ADDLs lead to neuron death (reviewed in ref *13*), which is highly selective with respect to nerve cell subtype (*13*, *14*) and appears to stem from an impact on signal transduction molecules (*8*, *15*).

Other subfibrillar species derived from A$\beta$ also are neuroactive. A$\beta$ dimers activate glial cells and can lead to nerve cell death in co-cultures containing astrocytes, but these dimers have no direct neurotoxicity (*16*). Direct action on neurons is evident, however, with preparations of protofibrils, which rapidly induce action potentials and other electrophysiological responses, and, with longer exposure, cause cell death (*9*, *10*). Protofibrils are the largest of the subfibrillar toxins, ranging to 400 nm in length and 1 000 000 Da in mass, and they appear to be intermediates on the pathway to amyloid fibril formation (*17*, *18*). Previous evidence has suggested that the various subfibrillar A$\beta$-derived toxins exist in vivo (*19*−*21*) and correlate well with brain dysfunction and degeneration in humans as well as transgenic mice (*22*−*24*). Recently, small soluble A$\beta$-oligomers characterized as equivalent to synthetic ADDLs have been found to accumulate in AD brain, with concentrations ranging up to 70-fold greater than in age-matched control brain tissue (*25*).

The current study concerns the formation, structure, and activity of ADDL molecules made in the absence of apoJ. Results show that globular, neurotoxic ADDLs are one of several outcomes possible from the spontaneous self-assembly of A$\beta_{1-42}$. These ADDLs are intrinsically stable molecules, not short-lived intermediates as might be inferred from the presence of ADDL-like structures in protofibril and fibril preparations (*6*, *10*). Their relative stability and neuronal impact support the hypothesis that ADDLs contribute significantly to AD pathogenesis and constitute useful targets for AD therapeutic intervention.

## EXPERIMENTAL PROCEDURES (MATERIALS AND METHODS)

*Chemicals and Reagents.* All chemicals were obtained from Sigma-Aldrich (St. Louis, MO) unless otherwise noted. Tissue culture reagents were obtained from CellGro (Media-Tech, Herndon, VA). Peptides were obtained from California Peptide (Napa, CA) or American Peptide (Sunnyvale, CA).

*Cell Culture.* PC12 rat pheochromacytoma cells (*26*) were maintained in F12K, 2.5% fetal calf serum (FCS), 15% heat-inactivated horse serum, and antibiotics (streptomycin, penicillin, and fungizone) (all from Gibco Invitrogen Corporation, Carlsbad, CA) in 6% $CO_2$. For all experiments, cells were plated at low density and grown to 70% confluence. Hippocampal cultures were prepared as previously described (*21*). Briefly, E18 rat hippocampi were removed and digested in papain (2 mg/mL, Sigma) for 30 min. Papain was removed and hippocampi were triturated with a fire-polished glass pipet. Cells were plated onto poly-L-lysine coated coverslips in 60 mm culture plates at a density of $5 \times 10^5$ cells per plate. Cultures were maintained in 5% $CO_2$, 37 °C incubator and medium was changed every week until treatment.

*A$\beta$-Derived Diffusible Ligand (ADDL) Preparation.* ADDLs were prepared according to Lambert et al. (*21*) (see also ref *27*). Briefly, solid A$\beta$ peptide was dissolved in cold hexafluoro-2-propanol (HFIP). The peptide was incubated at room temperature for at least 1 h to establish monomerization and randomization of structure. The HFIP was removed by evaporation, and the resulting peptide was stored as a film at −20 or −80 °C. The resulting film was dissolved in anhydrous DMSO at 5 mM and then diluted into the appropriate concentration and buffer (currently, 100 $\mu$M in phenol red-free F12) with vortexing. Next, the solution was aged 24 h at 4−8 °C. The sample was then centrifuged at 14000*g* for 10 min at 4−8 °C; the soluble oligomers were in the supernatant. Usually, a small pellet was observed, suggesting there was some pelletable material in 24 h aggregations. The supernatant was diluted 10−200-fold for experiments.

*Protein Assay.* A$\beta$ stock (2 mg/mL) or bovine serum albumin (2 mg/mL) was thawed, diluted 8-fold into F12 vehicle, and used for duplicate samples of a standard curve of 1, 2, 3, 4, and 5 $\mu$g/mL. The standards and unknowns were diluted to 20 $\mu$L with F12 vehicle before final dilution to 1 mL with $ddH_2O$. After addition of Coomassie Plus Protein Assay reagent (1 mL, Pierce Biotechnology, Inc., Rockford, IL), the samples were vortexed and read at 595 nm.

*MTT Reduction Assay.* Impairment of MTT reduction by ADDLs was as described (*21*). Briefly, PC12 cells were plated on 96-well collagen-coated plates and allowed to grow overnight. Cells were incubated with ADDLs for 4 h and then MTT was added for 4 h. Following the MTT reduction period, lysis buffer was added, and the plate was left overnight to enhance total formazan product liberation. Because the 96-well plate reader assay is susceptible to experimental variance, each condition was run at $N = 8$. Absorbance was measured at 550/690 nm or 570/690 nm.

*Atomic Force Microscopy (AFM).* AFM was carried out essentially as described (*28*). Samples containing A$\beta$ were prepared for AFM analysis by spotting 10 $\mu$L of solution onto freshly cleaved mica (Ted Pella, Inc., Redding, CA). Protein was allowed to adhere to the surface for 10 min at RT and then washed 2× with $ddH_2O$ to reduce background and eliminate salts and buffer contaminants. Captured images were obtained using the Nanoscope III Multimode Atomic Force Microscope (MMAFM) workstation (Digital Instruments, Santa Barbara, CA) using a "J"-type scanner with xy range of 150 $\mu$m. Tapping Mode (Digital Instruments) was employed for all images using etched silicon TESP Nanoprobes (Digital Instruments). At least four regions of the mica surface were examined to ensure that similar structures existed throughout the sample. Images presented here were top view subtracted images containing both height and error channel data. The amplitude channel (error channel) took the derivative of the height data to highlight the edges of features. These data were subtracted from the height data to improve resolution and image quality. Section analysis was accomplished by drawing a line over the individual globular species and measuring the distance from the mica surface to the top of the structure. This was done six times and an average was obtained.

*Native Gel Electrophoresis.* Fractions were diluted in native sample buffer (BioRad, Hercules, CA), loaded under native conditions onto precast 4−20% Tris-HCl gels (Bio-Rad) and electrophoresed in native buffer (Bio-Rad) at 100 V for 1.5−2.5 h at 4 °C. Following electrophoresis, gels were either electroblotted to Hybond-ECL nitrocellulose (Amersham Biosciences, Piscataway, NJ) at 100 V for 1 h at 4 °C

in transfer buffer (25 mM Tris-HCl, pH 8.3, 192 mM glycine, 20% v/v methanol) or silver stained (Silver Xpress silver staining kit; Invitrogen Corporation, Carlsbad, CA). Following the transfer, membranes were subjected to Western blotting (see below) using antibodies directed against the A$\beta$ peptide.

*SDS−PAGE and Western Blotting.* Protein samples (0.09−0.27 $\mu$g) were separated by electrophoresis at 100 V for 1 h, 45 min using 16.5% Tris-Tricine BioRad gels. Gels were then silver stained using 2× incubation times or transferred for immunoblotting. After transfer (1 h at 100 V at 4 °C) to Hybond ECL nitrocellulose, membranes were blocked in 5% nonfat dry milk in TBST (10 mM Tris-HCl, pH 7.4, 0.9% NaCl, 0.05% MgCl, and 0.1% Tween-20) for 1 h at RT. The membrane was then incubated with anti-A$\beta$ antibodies (6E10 and 4G8, Signet; 26D6, Sibia; M94 (*21*)) for 1.5 h at RT. Where noted, antibodies were used from mouse hybridoma cultures, which were generated by the Northwestern University Core Antibody Facility from mice injected seven times (30 $\mu$g of ADDLs/mouse/injection) over 5 months; positive hybridoma cultures were identified by dot blot and assessed by Western blot. Secondary antibodies conjugated to HRP (Amersham) were used to identify bound proteins. Proteins were visualized with chemiluminescence (Pierce, SuperSignal West femto) and quantified using film or Kodak 1D Image Analysis software for the Kodak IS440CF Image Station.

*2D (Native/SDS) PAGE.* ADDL preparations (50−100 pmol) were electrophoresed using the native polyacrylamide gel system of Betts et al. (*29*) (10%T acrylamide, 5%C resolving gels; 4.3%T, 5%C stacking gels) in a Bio-Rad mini Protean II apparatus at 120 V for approximately 3.5 h at 4 °C. A strip 2−3 mm wide was cut from the center of each sample lane and the gel equilibrated for 3−5 min in sample buffer (70 mM Tris-HCl, pH 6.8, 20% w/v glycerol, 2% w/v SDS, 0.0025% w/v bromphenol blue). The gel strip was electrophoresed in the second dimension by SDS−PAGE gel electrophoresis (*30*) (12%T acrylamide, 5%C resolving gel; 4.3%T, 5%C stacking gel) by pressing the gel strip onto the prepared SDS gel and sealing them together with 1% agarose (Seakem LE, FMC Corp., Rockland, ME) in sample buffer. The gel was run at 50 V for 30 min and 120 V for approximately 2 h at 4 °C. The 2D gels were analyzed by silver stain or Western blot using an anti-ADDLs antibody (Bethyl Laboratories, Inc., Montgomery, TX, M26) similar to those described previously (*21*).

*Temperature Jump Reorganization.* After ADDLs were made, the solution was diluted 10−100-fold into F12 media. Samples were either brought to 37 °C or left in the cold and incubated for 20 min to 24 h. Following the incubation, the samples were analyzed by electrophoresis and AFM.

*ERK Assay.* PC12 cells were plated at $1.5 \times 10^6$ cells/mL in collagen-coated 6-well dishes and allowed to grow overnight. The cells were then differentiated for 5 days using 100 ng/mL NGF. Cells were transferred to serum-free and NGF-free medium for 24 h. Cells were then stimulated with NGF (50 ng/mL, 10 min) with or without ADDLs (10 $\mu$M). In addition, some cells were pretreated with ADDLs for 1 h before stimulation with NGF as above. Cells were harvested in 150 mM NaCl, 1% deoxycholic acid, 0.1% SDS, 10 mM Tris, pH 7.2, 1 mM EGTA, 20 mM p-NPP, 50 $\mu$M sodium orthovanadate, and 1× complete protease inhibitor cocktail (*31*) by scraping, transferred to ultracentrifuge tubes, and lysed for 30 min. Lysates were clarified by ultracentrifugation (100000*g*, 4 °C, 1 h). The supernatant was separated and frozen at −80 °C until needed. Equal amounts of protein extract (5−10 $\mu$g) were added to an equal volume of Laemmli sample buffer (Bio-Rad, under nonreducing conditions), boiled for 5 min, and then centrifuged briefly. Samples were loaded onto 10% Tris-HCl gels (Bio-Rad) and SDS−PAGE carried out at 100 V. Proteins were transferred to nitrocellulose membrane as above. Membranes were blocked in 2% BSA/TBST for 1 h at RT. Membranes were then incubated in primary antibody (anti-active ERK, 1:5000 and anti-pan ERK, 1:10000; Promega, Madison, WI) for 1 h at RT. After washing of the membrane, secondary antibody (donkey anti-rabbit HRP-conjugated IgG, 1:10000, Amersham) was incubated with the membranes for 1 h at RT. Proteins were visualized with chemiluminescence and analyzed as described above.

*Rac Activation Assay.* PC12 cells were cultured on two collagen-coated 6-well dishes ($2 \times 10^6$ cells per well) in low serum medium (F12K, 1% fetal bovine serum, 1% antibiotic/antimycotic). After 18−24 h ($t = 0$), the medium in two wells was replaced with ADDLs (500 nM) or DMSO (0.6%) diluted in warm low serum medium to the indicated final concentration. At $t = 5$ min, this procedure was repeated for the remaining wells. At $t = 10$ min, the cells were washed once with PBS then suspended in the lysis buffer provided with the Rac Activation Assay kit (Cytoskeleton, Denver, CO). Duplicate wells were pooled. The lysates were processed and assayed for Rac1 activity according to the protocol provided by the manufacturer. The kit used "PAK−PBD Protein Beads" [PAK = p21 activated kinase 1 and PBD = p21 binding domain (also called CRIB region for Cdc42/Rac interactive binding region)]. PBD is 14 aa long (aa 74−88). The beads contained an 83-amino acid portion of PAK (aa 67−150). The PAK was also GST tagged.

*Dot Blot Assay.* ADDLs were prepared at 10 and 100 nM A$\beta$ in F12 with or without varied concentrations of *Ginkgo biloba* extract. An aliquot (2 $\mu$L) of each ADDL preparation was applied to nitrocellulose after the indicated incubation time. The membrane was then processed to determine the presence of ADDLs using the immunoblotting protocol described above for Western blotting. The *G. biloba* extracts were a gift of S. Moreau of Biomeasure Inc. (Milford, MA). EGb761 is a complex substance derived from the leaves of *G. biloba* plant. IPS 200 is the injectable formulation of EGb 761.

*Size Exclusion Chromatography (SEC).* ADDLs (∼14 nmol) were fractionated by the Äkta Explorer HPLC apparatus with a Superdex 75 HR 10/30 or a Superdex 200 HR 10/30 (Amersham Biosciences) column using ice cold F12 culture medium as the liquid phase at a flow rate of 0.4 mL/min. Fractions were collected in 300−500 $\mu$L aliquots. Columns were calibrated with at least four protein standards of known molecular weight spanning the column's separation range and void volume was established with blue dextran.

*ELISA.* Polyclonal anti-ADDLs IgG (Bethyl, M90, similar to ref *21*; 0.25 $\mu$g/well) in 20 mM Tris-HCl, pH 7.5, 0.8% w/v NaCl (TBS) was plated on Immulon 3 Removawell strips (Dynatech Labs, Chantilly, VA) for 2 h at RT. The wells were blocked with 3 × 250 $\mu$L of 2% BSA in TBS × 10 min at RT and 1 × 200 $\mu$L of 1% BSA in F12 for 1 h at 4

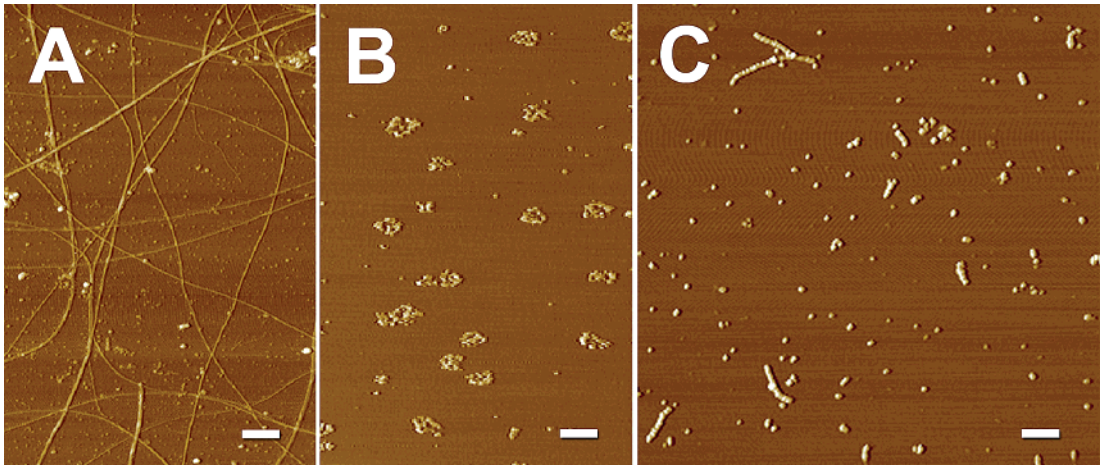


FIGURE 1: Diverse structural outcomes from different aggregation protocols. AFM images containing a spectrum of A$\beta$ structures are shown. (A) Fibrils: A$\beta_{1-42}$ aged in dd$H_2O$ for one week contains periodic and smooth fibrils throughout the field. Fibrils of diverse size and length are present. (B) Rings: A$\beta_{1-42}$ aged in F12 at 37 °C for 24 h and not centrifuged contains many ring-like structures. There are also a few short linear protofibrils present in this field. (C) ADDLs/protofibrils: A$\beta_{1-42}$ aged in PBS for 48 h at RT contains many linear protofibrillar structures and small, spherical structures. Protofibrillar structures appear to contain bead by bead assemblies of multiple globular structures. The line represents 400 nm in each panel. The results suggest that aggregation parameters of temperature and aggregation solution are critical for proper ADDLs formation.

°C. ADDLs (0.1−5 nM) and SEC peak fractions (1:300 dilution) in BSA/F12 were incubated 100 $\mu$L/well for 2 h at 4 °C followed by washing 3 × 10 min with BSA/TBS at RT. Monoclonal 6E10 was diluted 1:1500 in BSA/TBS and incubated 100 $\mu$L/well for 2 h at RT followed by washing as above. Biotinylated anti-mouse IgG (Vectastain ABC kit, Vector Labs, Burlingame, CA) was diluted 1:1000 in BSA/TBS and incubated 100 $\mu$L/well overnight at 4 °C followed by washing as above. An avidin−biotinylated-HRP complex (Vectastain ABC kit; 1:1000 dilution in BSA/TBS) was formed for 30 min and the complex incubated 100 $\mu$L/well for 75 min at RT. Following washing as above and rinsing 3× under running $dH_2O$, binding was visualized using 100 $\mu$L/well of Bio-Rad peroxidase substrate and read at 405 nm on a Dynex Technologies (Chantilly, VA) MRX-TC microplate reader.

*Immunocytochemistry*. Hippocampal cultures (18 DIV) were treated with 500 nM SEC peak fractions, nonpeak control, or unfractionated ADDLs at 37 °C, 5% $CO_2$ for 15 min. Cells were washed in Neurobasal medium and fixed with 3.7% formaldehyde for 40 min. Cells were washed in phosphate buffered saline (PBS), blocked with 10% normal goat serum (NGS) in PBS for 30 min. In parallel, cells from the groups mentioned above were permeabilized with 0.01% Triton X-100 in PBS/10%NGS for 30 min. Cells were then incubated with a rabbit A$\beta$ oligomer-generated polyclonal antibody M94 (*21*) at dilution of 1:5000 in PBS/10% NGS/0.01% Triton at 4 °C overnight. Cells were washed 3 × 10 min in PBS/1% NGS then incubated with Alexa Fluor488-conjugated anti-rabbit secondary antibody (Molecular Probes, Eugene, OR) at a dilution of 1:500 in PBS/1% NGS at RT for 2 h. Cells were washed 3 × 10 min in PBS, mounted on slides in a ProLong Antifade kit (Molecular Probes), and then imaged on a Leica Microsystems (Heidelberg, Germany) TCS SP2 confocal Scanner DMR XE7 microscope. Confocal images were collected using a 40× objective for image analysis. Filter cube I3 (excitation wavelength 450−490 nm) was used. Channel 1 was used to acquire M94-Alexa Fluor 488 immunofluorescence and channel 2 was used to acquire a Nomarski image using the transmitted light. A z-series scan at 0.5 $\mu$m intervals from individual fields was captured. Images presented are an overlay of channels 1 and 2.

## RESULTS

*A$\beta$ Peptide Self-Assembles into Multiple Alternative Structures.* A$\beta_{1-42}$ is an amphipathic peptide that readily self-associates into aggregates that are toxic to cultured cells. These structures can be imaged by atomic force microscopy (AFM), which detects not only large fibrils (Figure 1, panel A) but also subfibrillar assemblies such as rings (panel B), protofibrils, and ADDLs (panel C). Multiple structures often coexist, possibly consistent with precursor−product relationships. Varying lengths of rod-shaped protofibrils, e.g., are suggestive of beadlike addition of globular subunits, ranging from 2 to 15 in the micrograph shown here (panel C). Because A$\beta$ assembly leads to varying outcomes, it can be difficult to characterize the properties of a specific product such as ADDLs. However, the sensitive imaging of AFM provides a convenient means to assess structural homogeneity of a preparation.

*Preparation of Fibril-Free A$\beta$ Oligomers.* Analysis of conventional preparations of aggregated A$\beta$ indicates that multiple assembly pathways are energetically and kinetically accessible under typical laboratory conditions, resulting in formation of multiple structures. It is possible, however, to restrict assembly products to ADDLs by incubating A$\beta_{1-42}$ with apoJ (*8*), but because apoJ is difficult to obtain, we developed an alternative procedure (*21*, *27*) in which hexafluoro-2-propanol-(HFIP)-treated A$\beta_{1-42}$ is serially diluted into neat DMSO and then into cold F12 culture medium (Figure 2). When commercial peptide is suspended immediately in water or DMSO, fibrillar material forms rapidly because of seed structures (*32*), but HFIP appears to reduce or eliminate such seeds. AFM of A$\beta$ dried from HFIP shows no evidence of structures larger than 2 nm (*33*), consistent with the predominant monomer band seen in electrophoresis (Figure 2). The products obtained after 24 h in cold F12

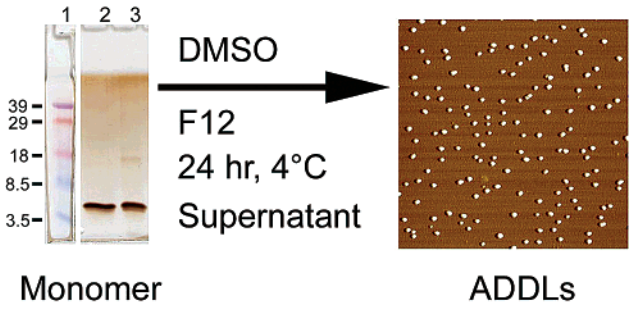


FIGURE 2: Spontaneous formation of ADDLs from pure monomeric A$\beta_{1-42}$. Panels show sequential stages of the ADDL preparation. Left: solid A$\beta$ peptide is dissolved in HFIP (5 mg/mL) for 1 h. HFIP is evaporated and the peptide film is resuspended in 100% HFIP or 10%HFIP/90%DMSO and separated by a silver-stained SDS−PAGE. The major species is A$\beta$ monomer, migrating to ~4.5 kDa. Lane 1: molecular weight markers. Lane 2: monomeric HFIP stock (100% HFIP). Lane 3: DMSO/HFIP stock (10% HFIP: 90% DMSO). Right: AFM image of ADDLs. DMSO stock is diluted into F12 (100 $\mu$M) and aged for 24 h at 5 °C. Following incubation and centrifugation, the supernatant is spotted onto freshly cleaved mica.

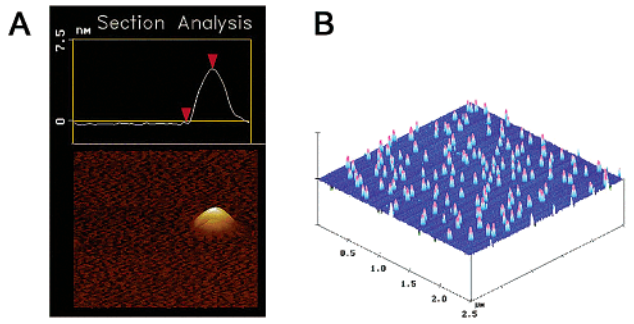


FIGURE 3: AFM shows ADDLs comprise globular oligomers of similar size. AFM images of ADDL preparations at higher and lower resolution are shown. (A) Section analysis of ADDLs was performed to determine the diameter of the oligomers. In this sample, the average Z height was found to be 5 nm. (B) AFM image of ADDLs contains primarily oligomers of A$\beta$, represented by the pink features. No fibrils or protofibrils are present in the solution represented here.

and brief centrifugation consist entirely of small globular molecules (confirmed independently in ref *34*). These were indistinguishable from ADDLs prepared in the presence of apoJ (*8*). F12 medium at low temperature was found suitable for ADDL formation even at relatively high monomer concentrations, distinguishing it from HEPES or phosphate buffered saline, where high monomer concentrations (100 $\mu$M) lead to a mixture of ADDLs and abundant rod-shaped protofibrils. When low concentrations of monomer (10−100 nM) are incubated in these buffers, only ADDLs are observed.

The globular nature of individual ADDL molecules was confirmed at higher AFM magnification, illustrated here by section analysis (Figure 3A). Z-height measurements gave a diameter of ~5 nm for the ADDLs shown, with diameters varying from 3 to 8 nm (mean of 5 ± 3 nm; SD). Globular structures of this size occurred only at very low levels in DMSO monomer solutions (not shown). Small soluble proteins gave Z-heights in the same range. Fibroblast growth factor (17 kDa), e.g., measured 3 ± 2 nm, and carbonic anhydrase (29 kDa) measured 4 ± 3 nm. Overall, the AFM analysis established that the ADDL preparations contained an abundance of small globular molecules not found in monomer stocks; further, these preparations were completely free of rod-shaped fibrils and protofibrils (Figure 3B; typical result from more than 50 preparations over a five-year period).

*ADDLs Are Heterogeneous.* Z-height measurements from AFM, although imprecise (as indicated, e.g., by fibroblast growth factor measurements), suggested possible heterogeneity of the globular ADDL molecules. Heterogeneity was confirmed by electrophoresis, which also verified the conclusion from AFM that ADDL preparations were free of large molecules (Figure 4). By native gel analysis (Figure 4A), ADDL solutions showed a major component that migrated near the 17 kDa standard (for reference only). Several minor bands, migrating faster as well as slower, were detectable by silver staining and Western blotting. Excision of the native gel lane and subsequent separation using SDS−PAGE (a 2D gel format) revealed that this major band contained trimer, tetramer, and pentamer (Figure 4D, middle). Minor amounts of monomer were observed when immunoblots used an antibody that recognizes monomer in addition to oligomers (Figure 4D, right). The faint, faster migrating band in the 1D native gel was exclusively monomer in the 2D analysis. A faint spectrum of higher molecular weight species also was evident (by immunoblotting, but not by silver stain). All species, however, entered the separating gel.

Assessment of size using standard denaturing gel conditions (1D SDS−PAGE), followed either by silver stain or immunoblotting, showed multiple bands whose size was consistent with discrete oligomeric forms of A$\beta$ (Figure 4B,C). Tetramer was prominent and higher molecular weight oligomers (through 24mer) also were seen (particularly in the immunoblots; differences between antibodies are considered later). Resolution of bands in ADDL preparations varied with buffer and gel composition (*33*). The results shown here were obtained by 16.5% Tris-tricine SDS−PAGE. Molecular weights from SDS−PAGE Tris-tricine gels ($n$ = 7) of the oligomer ladder gave discrete species derived from 4.5 kDa subunits of A$\beta$ monomer (data not shown), although the gel conditions were not optimal for analysis of higher molecular weight oligomers. The method used to make ADDLs for all experiments in the current study was chosen to provide relatively concentrated solutions, but less than the expected concentration for micelles, which tend to form at lower pH (*35*). Final A$\beta$ concentrations therefore were 25−100 $\mu$M. Oligomerization also can be attained using A$\beta$ concentrations as low as 10 nM (*36*).

*ADDLs at 37 °C Remain Oligomeric.* An important question was whether ADDLs prepared at 4 °C remained as globular oligomers when subjected to bioassay conditions of lower ADDL concentrations and physiological temperatures. ADDLs therefore were analyzed by AFM and electrophoresis after dilution in F12 culture medium (final A$\beta$ 1−10 $\mu$M) and incubation for 24 h at 37 °C. Under these bioassay conditions, ADDL solutions still showed no fibrillar structures (Figure 5A). Possible changes in size by AFM were not striking, but immunoblots following native gel electrophoresis (Figure 5B) indicated some decrease in the large band near the 17−22 kDa markers and an increase in slower migrating species. These changes were observed also by silver stain (not shown). When analyzed by SDS−PAGE (Figure 5C), the heated ADDLs showed a shift toward larger

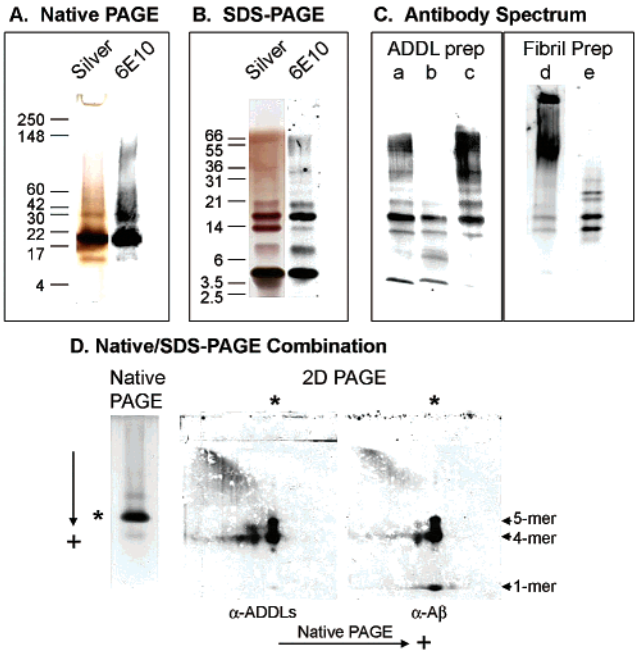


FIGURE 4: Electrophoretic analysis of ADDL solution shows presence of multiple oligomers. (A) ADDLs (~65 pmol/lane) were separated on a Tris-HCl polyacrylamide gel under native, nonreducing conditions and analyzed using silver stain and immunoblot procedures (see Methods). The silver stain and immunoblot (using 6E10 antibody) both show a large band near the 17 kDa marker (used for reference only), minor bands just before 17 kDa and between 22 and 30 kDa markers, and smears of other molecular weight structures. In addition, the immunoblot shows a broad band at higher molecular weight not found in the silver stain. (B) ADDLs were separated and analyzed as above, this time using denaturing, nonreducing conditions. The silver stain and immunoblot both show five major bands corresponding to monomer through pentamer species, with the higher oligomers through 24mer also evident. (C) ADDL and fibril preparations were separated using SDS−PAGE and immunoblot procedures (see above and Methods) and analyzed using different antibodies. (a) A monoclonal antibody to amino acids 3−12 of A$\beta$ sequence, 26D6, recognizes all of the putative oligomer species (monomer through 24mer). (b) A monoclonal antibody to amino acids 17−24 of A$\beta$ sequence, 4G8, recognizes primarily lower molecular weight oligomers, with a preference for dimer. (c) A new polyclonal antibody raised against oligomers, M94 (*21*), recognizes primarily higher molecular weight oligomer species, without recognizing monomer and dimer. (d) M94 polyclonal detects high molecular weight species (top of gel) and oligomers in fibril preparations. (e) Hybridoma-produced antibody detects only oligomers. (D**)** ADDLs were separated using native PAGE (left); this gel was transferred to a 2D gel for SDS−PAGE (see above and Methods). Analysis used the ADDL-selective polyclonal antibody M26 (middle, see Methods) and a monoclonal antibody that recognized total A$\beta$ (6E10, right). The major band seen in native analysis has monomer, slight trimer, tetramer, and pentamer. The leading band is exclusively monomer. The trailing band is primarily tetramer and pentamer.

oligomers, mostly 12/24mer species, but again, all material readily entered the separating gel. Whether analyzed by native or SDS gels, all material entered the separating gel. In contrast, preparations of protofibrils or fibrils (verified by AFM) aged under the same conditions contained material that was retained in the wells and stacking gel (see, e.g., Figure 4C-d). ADDLs incubated with cultured hippocampal neurons yielded oligomer profiles consistent with Figure 5 (not shown), with neither media nor cell extracts containing material excluded from gels. ADDLs once formed thus were relatively stable molecules that did not convert readily to

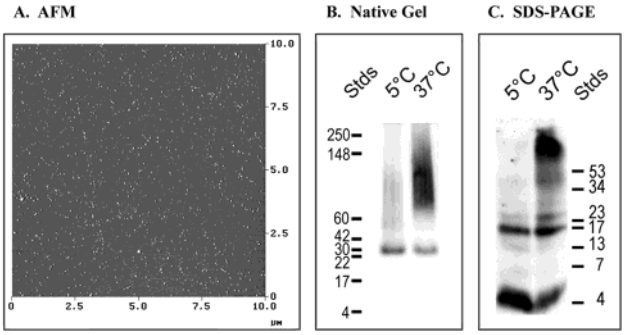


FIGURE 5: ADDLs remain oligomeric under bioassay conditions. (A) ADDLs were diluted to 1 $\mu$M, incubated an additional 24 h at 37 °C, and imaged by AFM. No protofibrils or fibrils are present in this preparation. (B) Native gel. ADDLs incubated for an additional 24 h at either 5 or 37 °C were analyzed on a 4−20% Tris-HCl gel using native, nonreducing conditions. The two lanes were immunoblotted using 26D6 antibody. The appearance of a smear between approximately 60 and 148 kDa indicates reorganization of the ADDLs into higher molecular weight oligomers but not into fibrillar or protofibrillar species. (C) Denaturing gel. ADDLs incubated as above were analyzed by immunoblot procedures on a 16.5% Tris-Tricine gel using denaturing, nonreducing conditions. The presence of oligomeric multiples of A$\beta$ are visible with both samples, but the sample maintained at 37 °C for an additional 24 h shows an increased amount of the 12mer and 24mer structures. Neither sample has immunoreactive material in the protofibrillar or fibrillar range.

protofibrils or larger assemblies, although fibrillar structures eventually can emerge following prolonged incubations (*34*).

*Bioactivity of Spontaneously Formed ADDLs.* Self-assembled ADDLs were tested for bioactivity with the PC12 pheochromacytoma cell line. The first tests assessed interference with MTT reduction, a measure of oxidative metabolism and vesicle trafficking (*37*). As previously reported for ADDLs made with apoJ, self-assembled ADDLs (1 $\mu$M total A$\beta$) caused a decrease in MTT reduction that was linear at low cell density (Figure 6A). The decrease occurred as early as 90 min (Figure 6B) and reached a plateau after 4−8 h incubation (not shown). For PC12 cells, the maximum impact was reached at concentrations slightly less than 5 $\mu$M total A$\beta$ (Figure 6C). Hippocampal primary cultures were more sensitive than PC12 cells to low doses of ADDLs, with a 35% decrease in MTT reduction seen at 50 and 100 nM peptide ($n = 8$ for each condition).

Two subsequent tests for ADDL bioactivity, again in PC12 cell culture, focused on short-term responses. We first investigated a possible impact on nerve growth factor (NGF) signaling. NGF alone, when added to cells for 10 min, caused a 10-fold increase in active ERKs (Figure 7A), similar to published reports (*38*). When ADDLs were added at the same time as NGF, phosphorylation was further stimulated (by 33 and 48% for ERK 42 and ERK 44, respectively). However, when cells were preincubated with ADDLs for 60 min before the addition of NGF, the response to NGF was greatly attenuated. ADDLs thus could enhance or decrease NGF-mediated signaling, depending on order of exposure. Total levels of ERKs in these experiments did not change (not shown). Activation of ERK by NGF in PC12 cells thus was rapidly perturbed by ADDLs.

Since previous work has shown a link between ADDL activity and Src-family kinases (Fyn; *8*), we next tested the effect of ADDLs on an upstream component of that signal transduction cascade, Rac 1. Activated Rac was isolated by

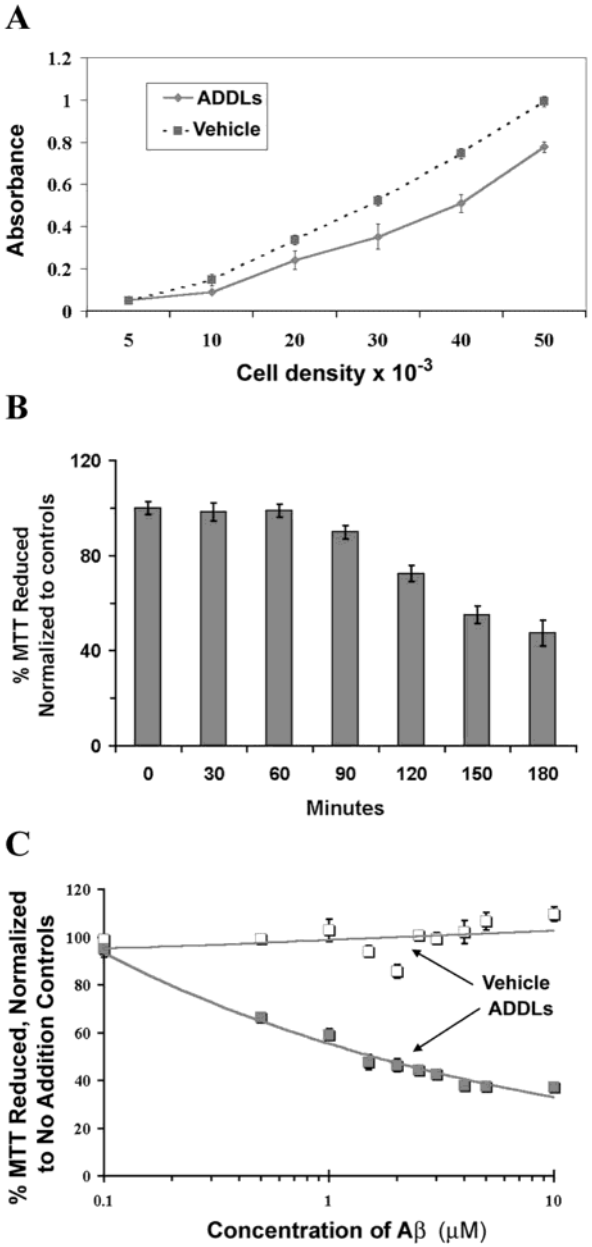


FIGURE 6: Spontaneously formed ADDLs cause decreased MTT reduction in PC12 cells. (A) PC12 cells were plated at the indicated cell number and allowed to grow overnight. After incubation of the sample with a 24 h ADDL preparation (1 $\mu$M) for 4 h, the MTT assay was performed (see Methods). (B) PC12 cells were plated at 30 000 cells/well and allowed to grow overnight. ADDLs (10 $\mu$M) were added for the indicated times before the MTT assay was performed. Toxicity levels became significant by 3 h. (C) PC12 cells (plated as above and grown overnight) were treated with ADDLs at the indicated concentrations for 4 h and assayed for toxicity (MTT assay). Results show ADDL toxicity in PC12 cells is linear, prominent within 3 h, and occurs at sub-micromolar doses of A$\beta$.

binding to the CRIB domain of the Rac effector protein PAK. Bound proteins were then separated by SDS−PAGE and visualized with a polyclonal anti-Rac antibody. PC12 cells incubated for 10 min with ADDLs showed a 15-fold increase in activated Rac1 compared to incubation with vehicle (Figure 7B). Rac stimulation was maximal at approximately 10 min and robust at low doses of ADDLs (50 nM). With respect to timing and dose, this cellular response to ADDLs is the most sensitive detected so far.

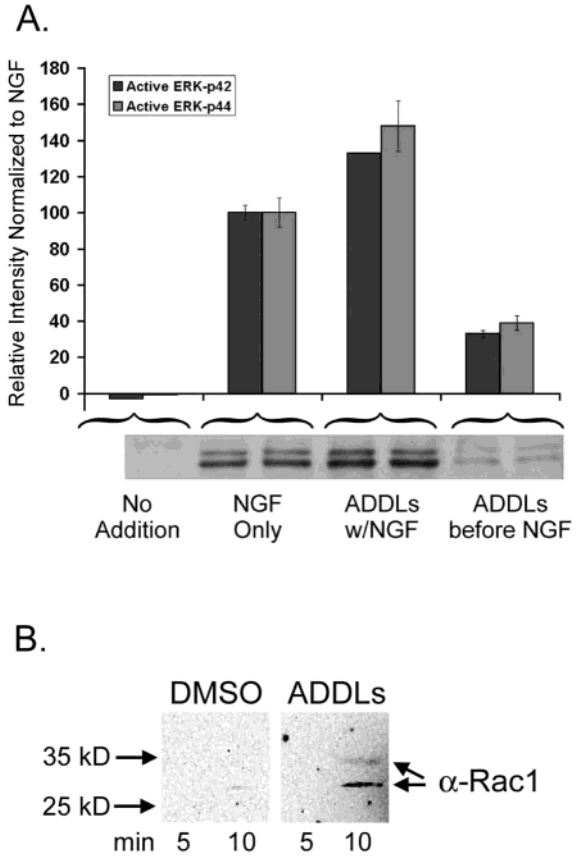


FIGURE 7: ADDLs alter NGF-dependent ERK stimulation and stimulate Rac1 in PC12 cells. (A) Quantitation of active ERKs is plotted above the original immunoblot data. By itself, NGF increases *active* ERKs p42/44 by 10-fold as expected. However, when ADDLs and NGF are added together, an additional increase of 33 and 48%, respectively, for p42 or p44 ERKs was observed. Pretreatment of PC12 cells with ADDLs followed by addition of NGF results in ERK activation only ~33% as high as that obtained with NGF alone. Total ERKs did not change upon addition of NGF, ADDLs, or both (data not shown), indicating that the effect was due to phosphorylation, not protein production. (B) PC12 cells were treated with ADDLs or vehicle for 5 or 10 min and then lysed with the commercial kit lysis buffer. Active Rac was then precipitated with agarose beads conjugated to the binding domain of the Rac effector protein PAK. The bound proteins were then separated and analyzed using SDS−PAGE and an anti-Rac polyclonal antibody. Data show that active Rac is induced by ADDLs after 10 min incubation.

*Anti-ADDL Action of Gingko biloba.* Given their bioactivity, ADDLs may prove good targets for therapeutic drugs. This possibility was suggested by a recent study of neuroprotective *G. biloba* (*39*), which was reported to lower A$\beta$ neurotoxicity and also appeared to inhibit ADDL formation. To verify whether *G. biloba* extracts block ADDL formation, we assessed their potency with sensitive dot immunoblotting that detects very low levels of oligomers within a milieu of monomer (*21*, *40*). ADDLs were made with and without two different formulations of the neuroprotective *G. biloba* extract. Both were found to retard formation of A$\beta$ oligomers (Figure 8), although the EGb form of the extract was more effective at retarding oligomer formation than the soluble form (IPS 200). EGb only partially blocked the bioactivity of ADDLs in the PC12 MTT assay, which is measured at relatively high ADDL doses (not shown). As can be seen in Figure 8, even at 100 nM A$\beta$, the extracts did not prevent oligomer formation with longer incubations. Protection by

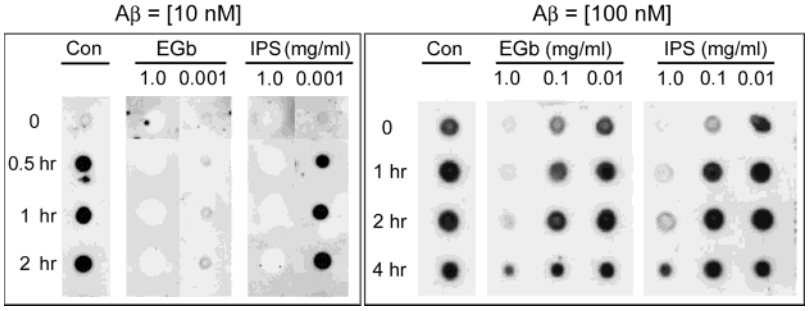


FIGURE 8: Neuroprotective extracts of *Ginkgo biloba* retard formation of A$\beta$ oligomers. Left: ADDLs (10 nM) were prepared with and without *Ginkgo biloba* extract (EGb) or the injectable form of the material (IPS) at the indicated concentrations. Aliquots were assayed for the presence of oligomers in a dot blot assay using an oligomer-selective antibody (see Methods). Both extracts retarded the formation of oligomers for up to 2 h at 1.0 mg/mL. Right: Both *Ginkgo biloba* extract (EGb) and the injectable form (IPS) at 1.0 mg/mL are also able to significantly block the formation of ADDLs at a higher concentration of A$\beta$ (100 nM).

*G. biloba* against low doses of A$\beta$, however, may be significant with respect to subtle effects at synapses, which have been suggested to alter memory function (*8*, *11*).

*Oligomers Have Conformationally Unique Epitopes.* Immunoblotting of ADDLs described above (Figure 4) was done with five antibodies: two monoclonals that recognize epitopes at the amino terminal of A$\beta$ (6E10, 26D6), a monoclonal that recognizes an internal A$\beta$ epitope (4G8), and two polyclonal antibodies that are oligomer-selective (M94, M26). The amino terminal antibodies, 26D6 (Figure 4C-a) and 6E10 (Figure 4B), identified oligomers up to the 24mer and had the greatest similarity to the silver-stained pattern. The internal epitope-directed 4G8 showed a high affinity for dimer and smaller oligomers (Figure 4C-b), but did not recognize higher molecular weight oligomers as avidly. The polyclonal antibodies M94 and M26, generated by vaccination with ADDLs (*21*), selectively bound oligomers rather than monomer or dimer. These antibodies can also recognize higher molecular weight A$\beta$ species (protofibrils and fibrils) if they are present (e.g., Figure 4C-d). The apparent differential accessibility of epitopes suggests possible conformational differences among the oligomers.

Differences in oligomer conformation of a different sort may be related to oligomer activity. As previously described for fibrils (*41*), some lots of synthetic A$\beta_{1-42}$ give minimal toxicity. The same situation is true for ADDL toxicity. For example, Figure 9a shows an ADDL preparation that had almost no impact on MTT reduction. Fortuitously, this particular inactive lot also was analyzed by gel electrophoresis. Silver stain profiles showed the presence of oligomers apparently equivalent to those found in toxic preparations (Figure 9b). However, immunoblots revealed distinguishing properties. The small oligomers seen by silver stain were not recognized by M94, a conformation-sensitive antibody generated by ADDL vaccination (*21*), even when overexposed (Figure 9c; compare with Figure 4C-c). The same blot stripped of M94 and reprobed with 6E10 monoclonal clearly showed the presence of immunoreactive oligomers (Figure 9d). This blot also showed dimer, typically a nonabundant species with little 6E10 immunoreactivity. Note that both 6E10 and M94 detect the trace high molecular weight species, but only 6E10 detects the trimers and tetramers. Thus, while M94 normally is highly reactive toward small molecular weight oligomers, it was unable to bind them in these nontoxic preparations, despite their demonstrated presence by silver stain and by 6E10. This result was

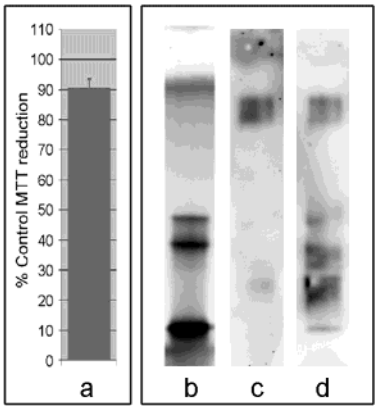


FIGURE 9: Immunoreactivity can discriminate active/inactive oligomers. (a) MTT assay (see Methods) of A$\beta$ lot that produced oligomers with low toxicity. Value is normalized to controls set at 100% reduction. (b) Silver stain of SDS−PAGE verifies that same A$\beta$ batch produced oligomer bands. (c) Immunoblot of inactive A$\beta$ batches with ADDL-selective antibody detects trace amounts of high MW material but only minimally detects the abundant small MW oligomers. (d) Stripping blot "C" and reprobing with 6E10 detects the high MW material but also detects multiple species of low molecular weight oligomers.

uncommon and was observed only one other time. It indicates, however, that same-sized oligomers thus can exist in different conformations, perhaps in a manner related to toxicity. The issue of conformation additionally has bearing on the relationship between small globular oligomers and large fibrils. A screen of hybridomas generated from ADDL-vaccinated mice produced one culture that secreted antibodies capable of binding oligomers but not fibrils (Figure 4C-e). These selective antibodies also detected ADDLs bound to hippocampal cells (not shown, but equivalent to Figure 10C), indicating that the bound species remained nonfibrillar.

Results comparing large and small oligomers separated by HPLC−SEC (peaks 1 and 2, respectively; Figure 10A) suggest that different oligomer conformation states also may occur in preparations that are toxic. Relative abundance of the two peaks varied between preparations, but their properties were consistent. Peak 1 elutes shortly after the void volume (75 kDa cutoff) and on native gels comprises a slow migrating species (inset, silver-stain 1). Peak 2 elutes near 13 kDa and on native gels comprises a faint band corresponding to monomer (inset, silver-stain 2) and a major band corresponding mostly to tetramer (asterisk, silver-stain 2; compare with Figure 4D). Solution properties of the two peaks were examined by sandwich ELISAs (Figure 10B) and

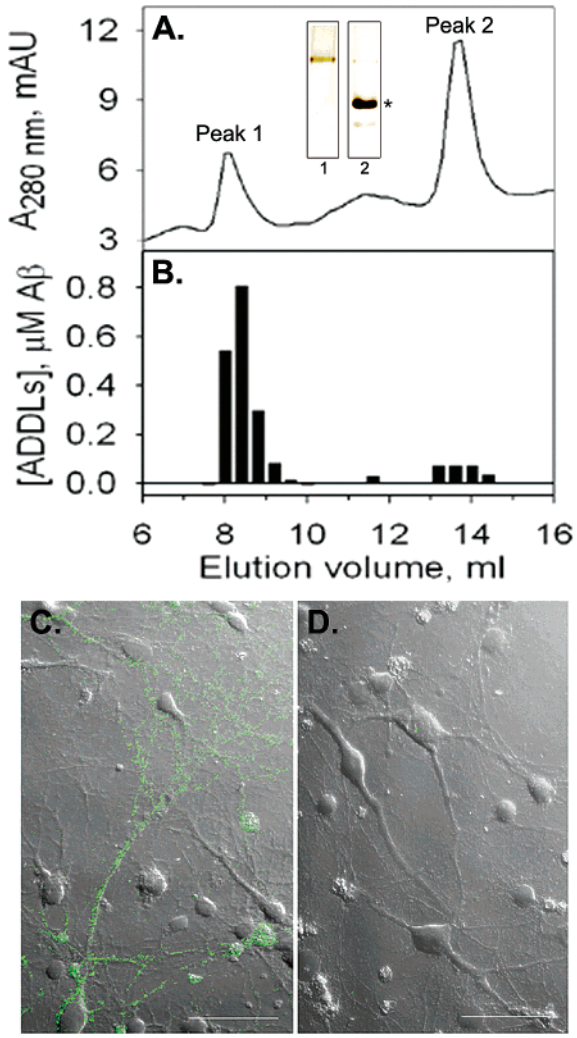


FIGURE 10: Large and small oligomers separated by HPLC−SEC exhibit distinct conformational characteristics. (A) ADDLs subjected to HPLC−SEC (Superdex 75 HR 10/30 column) produced two major peaks. Peak 1 elutes near the void volume and peak 2 elutes near 13 kDa. Silver-stained native gel confirmed the separation into large (inset, lane 1) and small oligomers (asterisk, lane 2). (B) A sandwich ELISA using ADDL-generated polyclonal antibodies to capture oligomers and a monoclonal antibody for detection showed higher sensitivity for the larger oligomers. Unfractionated ADDLs were used as a quantitative standard. (C and D) Immunofluorescence microscopy of embryonic rat hippocampal cultures demonstrated that large ADDLs bind selectively to the surface of cell bodies and processes at distinct puncta (identified as synapses; P. Lacor, unpublished) (C), while smaller ADDLs showed no cell labeling (D).

by specific binding to differentiated hippocampal neurons (Figure 10C,D). Oligomers in peak 1 were readily detected by both assays. In contrast, equal amounts of peak 2 provided minimal signal in ELISA and no binding to hippocampal neurons. Data suggest the hypothesis that tetramers in peak 2 exist in a conformation poorly recognized by antibody and not competent to assemble into larger oligomers.

## DISCUSSION

Since the initial report that A$\beta_{1-42}$ can form oligomers that are potent CNS neurotoxins (*8*), other studies have demonstrated that oligomer formation is a relatively general phenomenon applicable to multiple proteinopathies (*42*−*44*), including spongiform encephalopathies (prions; *45*) and Parkinson's (α-synuclein; *46*). Thus, while A$\beta$ oligomers are specifically relevant to AD, they may also provide a new paradigm for understanding the pathology associated with other proteinopathies where protein oligomer formation and toxicity can be documented.

The current paper confirms and extends our earlier studies on the assembly of A$\beta_{1-42}$ into a mixture of soluble, globular neurotoxic oligomers (ADDLs). Previous cell culture studies showed that small soluble A$\beta$ oligomers were neurotoxic at concentrations much lower than those seen with amyloid fibrils (*8*, *10*) and capable, moreover, of rapidly blocking long-term potentiation, a memory-associated type of synaptic information storage. More recently, chronic exposure to these oligomers has been shown to induce highly selective neurotoxicity in CA1 hippocampal neurons, with much reduced impact on adjacent CA3 neurons and no impact on cerebellar neurons (*14*), recapitulating the highly selective neuropathology manifest in AD. Further data implicating ADDLs in AD pathology have come from a recent study that found up to 70-fold higher concentrations of oligomers in AD brain tissue compared to aged-matched control brain tissue (*25*).

As established in the current study, the molecular weights of ADDLs formed in vitro are consistent with A$\beta$ trimer, tetramer, pentamer, and higher, up to a putative 24mer. Analyses by AFM and gel electrophoresis show that ADDLs are stable, independent entities rather than short-lived structures that rapidly convert into much larger assemblies such as protofibrils. Prolonged incubations (7 days) of concentrated ADDL preparations can lead to fibrillar structures (*34*), although it is clear that such large structures are not essential for bioactivity. When dilute solutions are incubated at 37 °C, the smaller trimeric and tetrameric ADDLs reorganize into larger (12−24mer) assemblies, but the solutions remain free of fibrils and protofibrils for at least 24 h. Although ADDL formation is known to be fostered by apoJ (*8*), the current results show this chaperone-like activity is not required for stable oligomerization. As with apoJ-fostered ADDLs, spontaneously formed ADDLs suppressed MTT reduction by PC12 cells. NGF stimulation of ERK phosphorylation also was suppressed. Toxicity inherent in stable A$\beta$ oligomers is consistent with their predicted role in AD, supported by recent findings that oligomer levels are elevated in AD brain (*25*, *27*, *47*). Neurotoxic A$\beta$ oligomers thus can be considered viable targets for therapeutic intervention. In a prototype assay for discovery of formation-blocking drugs, *G. biloba* extracts were confirmed (*39*) to retard aggregation of A$\beta$ monomer into oligomeric A$\beta$, particularly at low doses.

*Imaging Structures Assembled from A$\beta$.* The critical factor for obtaining preparations of neurotoxic oligomers on a consistent basis has been the ability to establish a starting A$\beta$ peptide that was exclusively monomeric, assessed using AFM and gel electrophoresis. Here, as in other studies (*48*), failure to eliminate fibril-nucleating seeds from the initial peptide solutions resulted in predominant fibril formation. Other reports have used sonication and filtration techniques for removal of such seeds from stock (*17*, *18*, *49*); however, we have found that HFIP pretreatment ensures more reproducible monomer production. HFIP has been used for solubilization of amylin (*50*) and prion (*51*) proteins, and it has been reported previously to enhance the α-helical content of the A$\beta$ peptide (*52*). This treatment effectively dissolves

higher order aggregates, eliminating fibril-forming "seeds" and erasing any "structural history" associated with previous peptide aggregation (*32*). SDS−PAGE (Figure 2) and AFM (not shown) established that the initial A$\beta$ solution in HFIP was monomer.

Aggregation of A$\beta_{1-42}$ peptide in cold F12 media resulted in SDS-stable oligomers that were structurally distinct from protofibrils. AFM images established the globular nature of the oligomeric structures and suggested possible heterogeneity. ADDLs congregate around an average Z height of 5 nm, which is similar to the Z height found for carbonic anhydrase, a globular protein of 29−40 kDa molecular mass. Globules of 5 nm diameter are consistent with structures that might contain 6−9 monomers of A$\beta$ (*53*). The average diameter is somewhat larger than expected for the prevalent tetramer/pentamer structures, due probably to the presence of oligomers as large as 24mers, which likely correspond to the largest 8 nm globules observed by AFM.

Aggregation of monomeric A$\beta_{1-42}$ in PBS generates a much broader range of structures including oligomers, protofibrils, and fibrils. The elongated, metastable protofibrils are rope-like structures reported to have diameters of 3-4 nm by AFM (*18*) and 6−8 nm via EM (*17*). Protofibrils appear to be valid, on-pathway intermediates in fibril formation (*10*, *49*) as they continue to aggregate to form insoluble fibrillar material similar to that found in plaques (*54*). Protofibrils form from A$\beta_{1-42}$ in PBS or HEPES regardless of HFIP treatment (data not shown; *17*, *33*). Ring-shaped structures, which were atypical for A$\beta$ (Figure 1B), were described earlier for $\alpha$-synuclein (*46*, *55*), and may be related to pore-like structures reported for A$\beta$ in bilayers (*56*).

*Electrophoretic Analysis of Composition and Structure.* Gel electrophoresis provided further evidence that ADDLs are oligomeric assemblies of A$\beta_{1-42}$ and confirmed that ADDL formation occurs under F12 medium conditions without formation of fibrillar or protofibrillar structures. Electrophoresis in denaturing gels revealed a spectrum of oligomers including dimers, trimers, tetramers, pentamers, and higher order oligomers up to 24mers. Native gel electrophoresis showed one major oligomeric species, sandwiched between two minor ones. Re-electrophoresis by SDS−PAGE in the second dimension resolved the major native band into tetramer and pentamer, with smaller amounts of monomer and trimer. The fainter, leading band in the native gels comprises exclusively monomer, while the slower migrating band is primarily tetramer and pentamer. Western blotting of denaturing gels with sensitive antibodies to ADDLs or A$\beta$ monomer epitopes revealed a broad spectrum of oligomers from dimer to 24mer, with tetramer appearing as the predominant structure. Although monomer is prevalent in the one-dimensional SDS−PAGE profiles, the two-dimensional native-SDS analyses revealed only small amounts of monomer in ADDL preparations, suggesting that SDS can dissociate some oligomers into monomer. Both native and SDS electrophoresis demonstrated that oligomer size distribution is dependent on time and temperature of incubation. When predominantly tetrameric ADDL preparations were warmed to 37 °C, the tetramer diminished and larger bands corresponding to 12mer and 24mer formed. No protofibrils or fibrils developed under these conditions (by AFM as well as gel electrophoresis). ADDLs thus exist as independent molecules for at least 24 h, sufficiently long-lived to account for the biological activity in these preparations. Whether ADDLs under some conditions aggregate to form protofibrils, as might be suggested by the incremental protofibril lengths seen in Figure 1C, remains to be determined.

SDS-stable oligomers are undetectable when the starting material is A$\beta_{1-40}$ (data not shown), although other studies using cross-linking of A$\beta_{1-40}$ show the presence of monomer, dimer, trimer, and tetramer assemblies which form in a pH-dependent process (*57*). Higher order oligomers also could be visualized in the high-concentration cross-linking of $I^{125}$ A$\beta_{1-40}$ with oligomeric glutaraldehyde (*58*). Very recent work with cross-linking of A$\beta_{1-42}$ indicates a different manner of oligomerization from A$\beta_{1-40}$, preferentially giving pentamer/hexamer species (*59*). It is possible that the formation of highly stable oligomers by A$\beta_{1-42}$ but not A$\beta_{1-40}$ is the underlying basis for the pathogenic role of A$\beta_{1-42}$.

Western blot detection of specific oligomers varied, depending on the particular antibody employed (Figures 4 and 9), suggesting conformational differences between aggregates that present unique epitopes for antibody generation. Antibodies raised to N-terminal peptide epitopes recognized all structures. The 4G8 antibody, raised to residues 17−25 of A$\beta$, was highly sensitive to dimer and recognized other small oligomers to some extent, but did not efficiently recognize the larger 12mer or 24mer structures. The ADDL-selective rabbit polyclonals M93 and M26 exhibited high selectivity for trimer, tetramer, and higher oligomers and poor recognition of monomer, similar to previously described rabbit polyclonal antibodies (*21*). Two oligomer preparations that unexpectedly showed little activity in the MTT bioassay did not show trimer/tetramer recognition by the ADDL-generated antibodies (Figure 9), suggesting that alternate, inactive assembly conformations may exist. Similar low reactivity toward ADDL-generated antibodies was evident for the small oligomer fraction obtained by SEC (Figure 10), suggesting that even in toxic preparations, oligomers might possibly assume alternate conformations.

*Biological Activity.* Consistent with the properties of apoJ-chaperoned ADDLs, the oligomeric A$\beta_{1-42}$ species produced in cold F12 were bioactive in PC12 cell assays. Impact was evident within 90 min when tested for suppressed reduction of MTT, an assay that measures vesicle trafficking and oxidative metabolism (*37*). Signal transduction events were perturbed even more quickly, as revealed by ADDL desensitization of ERK activation by NGF within 60 min. This effect is consistent with a recently reported effect of low, sublethal doses of A$\beta_{1-42}$ on CREB signaling in rat primary cortical cultures (*60*), known to be coupled to ERK signaling (*61*). A similar effect of A$\beta$ on MAPK and CREB in hippocampal slices also has been observed (*62*). The A$\beta_{1-42}$ solutions used in these studies were likely to contain oligomers, which form at nanomolar doses of monomer (*36*). The impact of ADDLs on ERK and, putatively, on CREB signaling may explain their ability to inhibit long-term potentiation (LTP), which has been documented in hippocampal slices (*8*, *63*) and in vivo (*2*, *64*) at low oligomer doses and in less than 1 h. Other toxic A$\beta$ species, in particular synthetic A$\beta_{1-40}$ protofibrils prepared at high concentrations, have not been linked to LTP inhibition, but can cause changes in membrane properties such as EPSPs,

action potentials, and membrane depolarization (*9*). ADDL treatment of PC12 cells also was found to rapidly stimulate Rac1 activity. This effect is intriguing because activated Rac is associated with synaptic spine growth (*65*), and ADDLs have been shown to bind specifically to synapses in hippocampal cell cultures (*66*). These effects add to the growing body of evidence that ADDLs act via specific signal transduction pathways, and they are fully consistent with the hypothesis that memory failure in early AD is a synaptic dysfunction attributable to soluble A$\beta$ oligomers (*8*, *11*, *13*).

*Link to Memory Failure: ADDLs as New Targets for Therapeutic Vaccines and Drugs.* The link between soluble forms of toxic A$\beta$ and memory impairment has been strengthened recently by results from multiple AD mouse models. In one study, mice overexpressing $\beta$−APP$_{751}$, that forms diffuse deposits but not plaques, exhibited age-dependent spatial learning deficits, suggesting that accumulation of soluble A$\beta$ assemblies was responsible (*67*). In another transgenic mouse that does express plaques, memory impairment correlated negatively with A$\beta_{insol}$ levels (*68*), with results implicating a soluble neurologically active species. Very recent studies demonstrated the presence of soluble A$\beta$ oligomers in older mice, which showed a correlation between oligomer levels and memory impairment (*24*). In related Tg mice, vaccination with aged A$\beta$ preparations, which are known to contain ADDLs, gave protection against age-onset memory deficits even though substantial insoluble A$\beta$ deposits remained (*69*), suggesting depletion of a soluble form of amyloid. In another study, multiple injections of A$\beta$ antibody reversed memory impairment in aged mice (*70*), independent of plaque reduction or of significant brain A$\beta$ reduction. Finally, passive vaccination of the PDAPP Tg mice with the anti-A$\beta$ monoclonal antibody m266 afforded dramatic reversal of memory failure within 24 h of a single antibody injection, again with no effect on plaque levels (*71*). A$\beta$/antibody complexes were found in the plasma and CSF of this mouse after immunization, leading to the supposition that m266 was clearing a nonfibril, nonmonomer, soluble A$\beta$ species. Use of antibodies that specifically target soluble A$\beta$ assemblies (a possibility suggested by Figure 4-e) may provide the memory benefits seen in transgenic mouse studies without the CNS inflammation observed in recent clinical vaccine trials (*72*); it is especially noteworthy that a subset of individuals in the same clinical trial actually did show striking cognitive benefits (*73*). Although not yet tested for memory benefits, protection against A$\beta$ pathology has been found in tg-mice given ibuprofen (*74*) or gelsolin (*75*), providing potential alternatives to antibody administration.

Since antibodies give reversal of memory deficits putatively by neutralizing A$\beta$ oligomers, it should be of value to identify small molecules capable of blocking oligomer assembly. The recent report (*39*) that neuroprotective extracts of *G. biloba* (EGb) could block ADDL assembly prompted our current experiments to confirm this effect. Previous studies had attributed the neuroprotective effects of EGb to putative antioxidant properties (*76*), but our results here using a sensitive immunoassay clearly indicate that the specific EGb fraction from *G. biloba* completely blocked ADDL assembly at 1.0 $\mu$g/mL, in harmony with the reported neuroprotection (*39*). Recently, we reported that submicromolar doses of certain functionalized cyclodextrins also can effectively block ADDL assembly and neurotoxicity (*36*, *40*). These findings suggest that ADDL blockade by small molecules could potentially lead to effective AD drugs. The present results, coupled with earlier findings of ADDL-selective antibodies (*21*), provide a strong rationale to target ADDLs as an effective Alzheimer's disease therapeutic and preventative strategy.

## REFERENCES


1. Lee, V. M., Goedert, M., and Trojanowski, J. Q. (2001) *Annu. Rev. Neurosci. 24*, 1121−1159.
2. Klein, W. L. (2000) in *Molecular Mechanisms of Neurodegenerative Diseases* (Chesselet, M. F., Ed.) pp 1−49, Humana Press, Inc., Totowa, New Jersey.
3. Selkoe, D. J., and Schenk, D. (2003) *Annu. Rev. Pharmacol. Toxicol. 43*, 545−584.
4. Pike, C. J., Walencewicz, A. J., Glabe, C. G., and Cotman, C. W. (1991) *Brain Res. 563*, 311−314.
5. Lorenzo, A., and Yankner, B. A. (1994) *Proc. Natl. Acad. Sci. U.S.A. 91*, 12243−12247.
6. Howlett, D. R., Jennings, K. H., Lee, D. C., Clark, M. S., Brown, F., Wetzel, R., Wood, S. J., Camilleri, P., and Roberts, G. W. (1995) *Neurodegeneration 4*, 23−32.
7. Hardy, J. A., and Higgins, G. A. (1992) *Science 256*, 184−185.
8. Lambert, M. P., Barlow, A. K., Chromy, B. A., Edwards, C., Freed, R., Liosatos, M., Morgan, T. E., Rozovsky, I., Trommer, B., Viola, K. L., Wals, P., Zhang, C., Finch, C. E., Krafft, G. A., and Klein, W. L. (1998) *Proc. Natl. Acad. Sci. U.S.A. 95*, 6448−6453.
9. Hartley, D. M., Walsh, D. M., Ye, C. P., Diehl, T., Vasquez, S., Vassilev, P. M., Teplow, D. B., and Selkoe, D. J. (1999) *J. Neurosci. 19*, 8876−8884.
10. Walsh, D. M., Hartley, D. M., Kusumoto, Y., Fezoui, Y., Condron, M. M., Lomakin, A., Benedek, G. B., Selkoe, D. J., and Teplow, D. B. (1999) *J. Biol. Chem. 274*, 25945−25952.
11. Hardy, J., and Selkoe, D. J. (2002) *Science 297*, 353−356.
12. Oda, T., Wals, P., Osterburg, H. H., Johnson, S. A., Pasinetti, G. M., Morgan, T. E., Rozovsky, I., Stine, W. B., Snyder, S. W., Holtzman, T. F., Krafft, G. A., and Finch, C. E. (1995) *Exp. Neurol. 136*, 22−31.
13. Klein, W. L., Krafft, G. A., and Finch, C. E. (2001) *Trends Neurosci. 24*, 219−224.
14. Kim, H. J., Chae, S. C., Lee, D. K., Chromy, B., Lee, S. C., Park, Y. C., Klein, W. L., Krafft, G. A., and Hong, S. T. (2003) *FASEB J. 17*, 118−120.
15. Longo, V. D., Viola, K. L., Klein, W. L., and Finch, C. E. (2000) *J. Neurochem. 75*, 1977−1985.
16. Roher, A. E., Chaney, M. O., Kuo, Y. M., Webster, S. D., Stine, W. B., Haverkamp, L. J., Woods, A. S., Cotter, R. J., Tuohy, J. M., Krafft, G. A., Bonnell, B. S., and Emmerling, M. R. (1996) *J. Biol. Chem. 271*, 20631−20635.
17. Walsh, D. M., Lomakin, A., Benedek, G. B., Condron, M. M., and Teplow, D. B. (1997) *J. Biol. Chem. 272*, 22364−22372.
18. Harper, J. D., Wong, S. S., Lieber, C. M., and Lansbury, P. T. (1997) *Chem. Biol. 4*, 119−125.
19. Kuo, Y. M., Emmerling, M. R., Vigo-Pelfrey, C., Kasunic, T. C., Kirkpatrick, J. B., Murdoch, G. H., Ball, M. J., and Roher, A. E. (1996) *J. Biol. Chem. 271*, 4077−4081.
20. Funato, H., Enya, M., Yoshimura, M., Morishima-Kawashima, M., and Ihara, Y. (1999) *Am. J. Pathol. 155*, 23−28.
21. Lambert, M. P., Viola, K. L., Chromy, B. A., Chang, L., Morgan, T. E., Yu, J., Venton, D. L., Krafft, G. A., Finch, C. E., and Klein, W. L. (2001) *J. Neurochem. 79*, 595−605.
22. Lue, L. F., Kuo, Y. M., Roher, A. E., Brachova, L., Shen, Y., Sue, L., Beach, T., Kurth, J. H., Rydel, R. E., and Rogers, J. (1999) *Am. J. Pathol. 155*, 853−862.
23. McLean, C. A., Cherny, R. A., Fraser, F. W., Fuller, S. J., Smith, M. J., Beyreuther, K., Bush, A. I., and Masters, C. L. (1999) *Ann. Neurol. 46*, 860−866.
24. Westerman, M. A., Chang, L., Frautschy, S., Kotilinek, L., Cole, G., Klein, W., and Hsiao Ashe, K. (2002) Ibuprofen reverses memory loss in transgenic mice modeling Alzheimer's disease. *Soc. Neurosci. Abstr. 28*, 690.4.
25. Gong, Y., Chang, L., Viola, K. L., Lacor, P. N., Lambert, M. P., Finch, C. E., Krafft, G. A., and Klein, W. L. (2003) *Proc. Natl. Acad. Sci. U.S.A. 100*, 10417−10422.
26. Greene, L. A., and Tischler, A. S. (1976) *Proc. Natl. Acad. Sci. U.S.A. 73*, 2424−2428.
27. Klein, W. L. (2002) *Neurochem. Int. 41*, 345−352.

28. Stine, W. B., Jr., Snyder, S. W., Ladror, U. S., Wade, W. S., Miller, M. F., Perun, T. J., Holzman, T. F., and Krafft, G. A. (1996) *J. Protein Chem. 15*, 193−203.
29. Betts, S., Speed, M., and King, J. (1999) *Methods Enzymol. 309*, 333−350.
30. Laemmli, U. K. (1970) *Nature 227*, 680−685.
31. Berg, M. M., Krafft, G. A., and Klein, W. L. (1997) *J. Neurosci. Res. 50*, 979−989.
32. Dahlgren, K. N., Manelli, A. M., Stine, W. B., Jr., Baker, L. K., Krafft, G. A., and LaDu, M. J. (2002) *J. Biol. Chem. 277*, 32046−32053.
33. Chromy, B. (2001) Characterization of Toxic Abeta Oligomers (ADDLs, Amyloid-Beta-Derived-Diffusible Ligands): A New Theory in Alzheimer's Disease Causation. 1−288, Northwestern University Dissertation.
34. Stine, W. B., Jr., Dahlgren, K. N., Krafft, G. A., and LaDu, M. J. (2003) *J. Biol. Chem. 278*, 11612−11622.
35. Lomakin, A., Chung, D. S., Benedek, G. B., Kirschner, D. A., and Teplow, D. B. (1996) *Proc. Natl. Acad. Sci. U.S.A. 93*, 1125−1129.
36. Yu, J., Bakhos, L., Chang, L., Holterman, M. J., Klein, W. L., and Venton, D. L. (2002) *J. Mol. Neurosci. 19*, 51−55.
37. Liu, Y., Peterson, D. A., and Schubert, D. (1998) *Proc. Natl. Acad. Sci. U.S.A. 95*, 13266−13271.
38. Xia, Z., Dickens, M., Raingeaud, J., Davis, R. J., and Greenberg, M. E. (1995) *Science 270*, 1326−1331.
39. Yao, Z., Drieu, K., and Papadopoulos, V. (2001) *Brain Res. 889*, 181−190.
40. Chang, L., Bakhos, L., Wang, Z., Venton, D. L., and Klein, W. L. (2003) *J. Mol. Neurosci. 20*, 305−314.
41. May, P. C., Gitter, B. D., Waters, D. C., Simmons, L. K., Becker, G. W., and Small, J. S. (1992) *Neurobiol. Aging 13*, 605−607.
42. El Agnaf, O. M. A., Nagala, S., Patel, B. P., and Austen, B. M. (2001) *J. Mol. Biol. 310*, 157−168.
43. Bucciantini, M., Giannoni, E., Chiti, F., Baroni, F., Formigli, L., Zurdo, J., Taddei, N., Ramponi, G., Dobson, C. M., and Stefani, M. (2002) *Nature 416*, 507−511.
44. Kirkitadze, M. D., Bitan, G., and Teplow, D. B. (2002) *J. Neurosci. Res. 69*, 567−577.
45. Baskakov, I. V., Legname, G., Baldwin, M. A., Prusiner, S. B., and Cohen, F. E. (2002) *J. Biol. Chem. 277*, 21140−21148.
46. Conway, K. A., Lee, S. J., Rochet, J. C., Ding, T. T., Williamson, R. E., and Lansbury, P. T., Jr. (2000) *Proc. Natl. Acad. Sci. U.S.A. 97*, 571−576.
47. Kayed, R., Head, E., Thompson, J. L., McIntire, T. M., Milton, S. C., Cotman, C. W., and Glabe, C. G. (2003) *Science 300*, 486-489.
48. Koo, E. H., Lansbury, P. T., Jr., and Kelly, J. W. (1999) *Proc. Natl. Acad. Sci. U. S.A. 96*, 9989−9990.
49. Harper, J. D., Wong, S. S., Lieber, C. M., and Lansbury, P. T., Jr. (1999) *Biochemistry 38*, 8972−8980.
50. Nilsson, M. R., Nguyen, L. L., and Raleigh, D. P. (2001) *Anal. Biochem. 288*, 76−82.
51. Wille, H., Prusiner, S. B., and Cohen, F. E. (2000) *J. Struct. Biol. 130*, 323−338.
52. Barrow, C. J., Yasuda, A., Kenny, P. T., and Zagorski, M. G. (1992) *J. Mol. Biol. 225*, 1075−1093.
53. Schneider, S. W., Larmer, J., Henderson, R. M., and Oberleithner, H. (1998) *Pflugers Arch. 435*, 362−367.
54. Blackley, H. K. L., Sanders, G. H. W., Davies, M. C., Roberts, C. J., Tendler, S. J. B., and Wilkinson, M. J. (2000) *J. Mol. Biol. 298*, 833−840.
55. Volles, M. J., Lee, S. J., Rochet, J. C., Shtilerman, M. D., Ding, T. T., Kessler, J. C., and Lansbury, P. T., Jr. (2001) *Biochemistry 40*, 7812−7819.
56. Lashuel, H. A., Petre, B. M., Wall, J., Simon, M., Nowak, R. J., Walz, T., and Lansbury, P. T., Jr. (2002) *J. Mol. Biol. 322*, 1089−1102.
57. Bitan, G., Lomakin, A., and Teplow, D. B. (2001) *J. Biol. Chem. 276*, 35176−35184.
58. Levine, H. (1995) *Neurobiol. Aging 16*, 755−764.
59. Bitan, G., Kirkitadze, M. D., Lomakin, A., Vollers, S. S., Benedek, G. B., and Teplow, D. B. (2003) *Proc. Natl. Acad. Sci. U.S.A. 100*, 330−335.
60. Tong, L., Thornton, P. L., Balazs, R., and Cotman, C. W. (2001) *J. Biol. Chem. 276*, 17301−17306.
61. Sweatt, J. D. (2001) *J. Neurochem. 76*, 1−10.
62. Dineley, K. T., Westerman, M., Bui, D., Bell, K., Ashe, K. H., and Sweatt, J. D. (2001) *J. Neurosci. 21*, 4125−4133.
63. Wang, H. W., Pasternak, J. F., Kuo, H., Ristic, H., Lambert, M. P., Chromy, B., Viola, K. L., Klein, W. L., Stine, W. B., Krafft, G. A., and Trommer, B. L. (2002) *Brain Res. 924*, 133−140.
64. Walsh, D. M., Klyubin, I., Fadeeva, J. V., Cullen, W. K., Anwyl, R., Wolfe, M. S., Rowan, M. J., and Selkoe, D. J. (2002) *Nature 416*, 535−539.
65. Nakayama, A. Y., and Luo, L. (2000) *Hippocampus 10*, 582−586.
66. Lacor, P. N., Viola, K. L., Lambert, M. P., Finch, C. E., Krafft, G. A., and Klein, W. L. (2002) Synapse homeostasis, its disruption by soluble Abeta oligomers, and reversal of memory loss in Alzheimer's disease. *Soc. Neurosci. Abstr. 28*, 751.7.
67. Koistinaho, M., Ort, M., Cimadevilla, J. M., Vondrous, R., Cordell, B., Koistinaho, J., Bures, J., and Higgins, L. S. (2001) *Proc. Natl. Acad. Sci. U.S.A. 98*, 14675−14680.
68. Westerman, M. A., Cooper-Blacketer, D., Mariash, A., Kotilinek, L., Kawarabayashi, T., Younkin, L. H., Carlson, G. A., Younkin, S. G., and Ashe, K. H. (2002) *J. Neurosci. 22*, 1858−1867.
69. Morgan, D., Diamond, D. M., Gottschall, P. E., Ugen, K. E., Dickey, C., Hardy, J., Duff, K., Jantzen, P., DiCarlo, G., Wilcock, D., Connor, K., Hatcher, J., Hope, C., Gordon, M., and Arendash, G. W. (2000) *Nature 408*, 982−985.
70. Kotilinek, L. A., Bacskai, B., Westerman, M., Kawarabayashi, T., Younkin, L., Hyman, B. T., Younkin, S., and Ashe, K. H. (2002) *J. Neurosci. 22*, 6331−6335.
71. Dodart, J. C., Bales, K. R., Gannon, K. S., Greene, S. J., DeMattos, R. B., Mathis, C., DeLong, C. A., Wu, S., Wu, X., Holtzman, D. M., and Paul, S. M. (2002) *Nat. Neurosci. 5*, 452−457.
72. Birmingham, K., and Frantz, S. (2002) *Nat. Med. 8*, 199−200.
73. Hock, C., Konietzko, U., Streffer, J. R., Tracy, J., Signorell, A., Muller-Tillmanns, B., Lemke, U., Henke, K., Moritz, E., Garcia, E., Wollmer, M. A., Umbricht, D., de Quervain, D. J., Hofmann, M., Maddalena, A., Papassotiropoulos, A., and Nitsch, R. M. (2003) *Neuron 38*, 547−554.
74. Lim, G. P., Yang, F., Chu, T., Gahtan, E., Ubeda, O., Beech, W., Overmier, J. B., Hsiao-Ashe, K., Frautschy, S. A., and Cole, G. M. (2001) *Neurobiol. Aging 22*, 983−991.
75. Matsuoka, Y., Saito, M., LaFrancois, J., Saito, M., Gaynor, K., Olm, V., Wang, L., Casey, E., Lu, Y., Shiratori, C., Lemere, C., and Duff, K. (2003) *J. Neurosci. 23*, 29−33.
76. Bastianetto, S., Ramassamy, C., Dore, S., Christen, Y., Poirier, J., and Quirion, R. (2000) *Eur. J. Neurosci. 12*, 1882−1890.


BI030029Q